SOCIETY FOR SCIENCE AND EDUCATION UNITED KINGDOM
TMLAI TRANSACTIONS ON MACHINE LEARNING AND ARTIFICIAL INTELLIGENCE
VOLUME 3, ISSUE 5
ISSN 2054-7390

Simulation of the Charge Motion near the Velocity of Light in Electric and Magnetic Fields

[1] Masami Morooka and [2] Midori Morooka-Sugiura
[1]Department of Electrical Engineering, Fukuoka Institute of Technology, Fukuoka, Japan;
[2]Flash Design Center, Micron Japan, Tokyo, Japan;
morooka@fit.ac.jp

ABSTRACT

A numerical simulation method for the charge motion near the velocity of light in electric and magnetic fields has been investigated using the relativistic mass by Einstein's special theory of relativity, and an electron acceleration for the Larmor motion in a static magnetic field perpendicularly applied a synchronized alternative electric field has been simulated by Java programing. The simulation results in a limitation of the electron velocity to a considerably lower value than the velocity of light in contradiction to the previous simulation in which the electron is easily accelerated over the velocity of light due to the use of the invariant mass.

Keywords: Simulation of charge motion near the velocity of light in electric and magnetic fields, Java programming, simulation of charge motion with the relativistic mass.

1 Introduction

The authors previously proposed a Java simulation for the rapid and accurate image learning of the charge motion in electric and magnetic fields using the Runge-Kutta method [1, 2]. In this simulation, we use an invariant mass of the charge resulting in an easy acceleration of the electron over the velocity of light for the Larmor motion in a static magnetic field applied a synchronized alternative electric field perpendicularly to the magnetic field. It is not accurate to use the invariant mass for the particle moving with a large momentum, and the relativistic mass by Einstein's special theory of relativity should be used in such a case. That is, the particle moving with a velocity near the velocity of light behaves effectively as a particle with a larger mass that increases with the increase in the velocity. This change of the effective mass causes a slip off of the above Larmor motion from the initial synchronization, resulting in a limitation of the acceleration and velocity.

In this paper, the numerical simulation method for the charge motion near the velocity of light in electric and magnetic fields has been investigated using the relativistic mass. Furthermore, the acceleration for the Larmor motion of electron in a static magnetic field applied the synchronized electric field has been simulated in comparison with the previous simulation used the invariant mass.

DOI: 10.14738/tmlai.35.1580
Publication Date: 31st October, 2015
URL: http://dx.doi.org/10.14738/tmlai.35.1580

2 Numerical Method for Charge Motion near the Velocity of Light in Electric and Magnetic Fields

2.1 Equations for the Charge Motion near the Velocity of Light in Electric and Magnetic Fields

The particle moving with a very large velocity $\boldsymbol{v}$ = (v_x, v_y, v_z) has a large momentum and thus behaves effectively as a particle with a large relativistic mass, m^*, according to Einstein's special theory of relativity. In this situation, the acceleration $\boldsymbol{a}$ under a force $\boldsymbol{F}$, $\boldsymbol{a} = d\boldsymbol{v}/dt$, is obtained as in Reference [3]:

$$\boldsymbol{a} = \frac{\boldsymbol{F} - (\boldsymbol{F} \bullet \boldsymbol{v})\boldsymbol{v} / c^2}{m\gamma}. \tag{1}$$

Here, m is the invariant mass, c is the velocity of light, and

$$\gamma = \frac{1}{\sqrt{1 - (v/c)^2}}. \tag{2}$$

Here, v is the magnitude of $\boldsymbol{v}$. Equation (1) represents the well-known Lorentz's longitudinal and transverse masses, that is, $m^*_{L} = m\gamma^{\square}$ when $\boldsymbol{F}$ is parallel to $\boldsymbol{v}$ and $m^*_{T} = m\gamma$ when $\boldsymbol{F}$ is perpendicular to $\boldsymbol{v}$□

We consider a motion of the charge q under the electric field, $\boldsymbol{E}$ = (E_x, E_y, E_z), and the magnetic field, $\boldsymbol{B}$ = (B_x, B_y, B_z). In this case, the acceleration is given as

$$\boldsymbol{a} = \frac{q\boldsymbol{E}}{m\gamma^3} + \frac{q\boldsymbol{v} \times \boldsymbol{B}}{m\gamma}. \tag{3}$$

Because the electric force is effective on the parallel component of $\boldsymbol{v}$ and the electro-magnetic force is perpendicular to $\boldsymbol{v}$. We have the equation for the displacement of the charge, $\boldsymbol{r}$ = (x, y, z):

$$\frac{d\boldsymbol{r}}{dt} = \boldsymbol{v}. \tag{4}$$

By decomposing the vector equations (3) and (4) into the scalar equations in the x, y, and z directions, we obtain

$$\frac{dv_x}{dt} = \frac{q}{m\gamma^3}E_x + \frac{q}{m\gamma}(v_y B_z - v_z B_y), \tag{5}$$

$$\frac{dv_y}{dt} = \frac{q}{m\gamma^3}E_y + \frac{q}{m\gamma}(v_z B_x - v_x B_z), \tag{6}$$

$$\frac{dv_z}{dt} = \frac{q}{m\gamma^3}E_z + \frac{q}{m\gamma}(v_x B_y - v_y B_x), \tag{7}$$

$$\frac{dx}{dt}=v_x, \tag{8}$$

$$\frac{dy}{dt}=v_y, \tag{9}$$

$$\frac{dz}{dt}=v_z. \tag{10}$$

We can obtain the charge motion in the *x*, *y*, and *z* directions by solving six ordinary differential equations, (5) - (10).

2.2 Numerical Method

The ordinary differential equations can be solved numerically using the fourth-order Runge-Kutta method. The first-order increment functions for the differential equations (5) – (10) at the known variables (t, v_x, v_y, v_z, x, y, z) are given as

$$k_1^{(1)}=\frac{q}{m}\left(1-(v_x^2+v_y^2+v_z^2)/c^2\right)^{1.5}E_x(t)+\frac{q}{m}\sqrt{1-(v_x^2+v_y^2+v_z^2)/c^2}\left(v_yB_z(t)-v_zB_y(t)\right), \tag{11}$$

$$k_2^{(1)}=\frac{q}{m}\left(1-(v_x^2+v_y^2+v_z^2)/c^2\right)^{1.5}E_y(t)+\frac{q}{m}\sqrt{1-(v_x^2+v_y^2+v_z^2)/c^2}\left(v_zB_x(t)-v_xB_z(t)\right), \tag{12}$$

$$k_3^{(1)}=\frac{q}{m}\left(1-(v_x^2+v_y^2+v_z^2)/c^2\right)^{1.5}E_z(t)+\frac{q}{m}\sqrt{1-(v_x^2+v_y^2+v_z^2)/c^2}\left(v_xB_y(t)-v_yB_x(t)\right), \tag{13}$$

$$k_4^{(1)}=v_x, \tag{14}$$

$$k_5^{(1)}=v_y, \tag{15}$$

$$k_6^{(1)}=v_z. \tag{16}$$

The second-order increment functions are given as

$$k_1^{(2)}=\frac{q}{m}\left(1-[(v_x+\frac{hk_1^{(1)}}{2})^2+(v_y+\frac{hk_2^{(1)}}{2})^2+(v_z+\frac{hk_3^{(1)}}{2})^2]/c^2\right)^{1.5}E_x(t+\frac{h}{2})$$

$$+\frac{q}{m}\sqrt{1-[(v_x+\frac{hk_1^{(1)}}{2})^2+(v_y+\frac{hk_2^{(1)}}{2})^2+(v_z+\frac{hk_3^{(1)}}{2})^2]/c^2}\left((v_y+\frac{hk_2^{(1)}}{2})B_z(t+\frac{h}{2})-(v_z+\frac{hk_3^{(1)}}{2})B_y(t+\frac{h}{2})\right), \tag{17}$$

$$k_2^{(2)} = \frac{q}{m}\left(1 - [(v_x + \frac{hk_1^{(1)}}{2})^2 + (v_y + \frac{hk_2^{(1)}}{2})^2 + (v_z + \frac{hk_3^{(1)}}{2})^2] / c^2\right)^{1.5} E_y(t + \frac{h}{2})$$

$$+\frac{q}{m}\sqrt{1 - [(v_x + \frac{hk_1^{(1)}}{2})^2 + (v_y + \frac{hk_2^{(1)}}{2})^2 + (v_z + \frac{hk_3^{(1)}}{2})^2] / c^2}\left((v_z + \frac{hk_3^{(1)}}{2})B_x(t + \frac{h}{2}) - (v_x + \frac{hk_1^{(1)}}{2})B_z(t + \frac{h}{2})\right), \qquad (18)$$

$$k_3^{(2)} = \frac{q}{m}\left(1 - [(v_x + \frac{hk_1^{(1)}}{2})^2 + (v_y + \frac{hk_2^{(1)}}{2})^2 + (v_z + \frac{hk_3^{(1)}}{2})^2] / c^2\right)^{1.5} E_z(t + \frac{h}{2})$$

$$+\frac{q}{m}\sqrt{1 - [(v_x + \frac{hk_1^{(1)}}{2})^2 + (v_y + \frac{hk_2^{(1)}}{2})^2 + (v_z + \frac{hk_3^{(1)}}{2})^2] / c^2}\left((v_x + \frac{hk_1^{(1)}}{2})B_y(t + \frac{h}{2}) - (v_y + \frac{hk_2^{(1)}}{2})B_x(t + \frac{h}{2})\right), \qquad (19)$$

$$k_4^{(2)} = v_x + \frac{hk_1^{(1)}}{2}, \qquad (20)$$

$$k_5^{(2)} = v_y + \frac{hk_2^{(1)}}{2}, \qquad (21)$$

$$k_6^{(2)} = v_z + \frac{hk_3^{(1)}}{2}. \qquad (22)$$

The third-order increment functions are given as

$$k_1^{(3)} = \frac{q}{m}\left(1 - [(v_x + \frac{hk_1^{(2)}}{2})^2 + (v_y + \frac{hk_2^{(2)}}{2})^2 + (v_z + \frac{hk_3^{(2)}}{2})^2] / c^2\right)^{1.5} E_x(t + \frac{h}{2})$$

$$+\frac{q}{m}\sqrt{1 - [(v_x + \frac{hk_1^{(2)}}{2})^2 + (v_y + \frac{hk_2^{(2)}}{2})^2 + (v_z + \frac{hk_3^{(2)}}{2})^2] / c^2}\left((v_y + \frac{hk_2^{(2)}}{2})B_z(t + \frac{h}{2}) - (v_z + \frac{hk_3^{(2)}}{2})B_y(t + \frac{h}{2})\right), \qquad (23)$$

$$k_6^{(3)} = v_z + \frac{hk_3^{(2)}}{2}. \qquad (24)$$

The fourth-order increment functions are given as

$$k_1^{(4)} = \frac{q}{m}\left(1 - [(v_x + hk_1^{(3)})^2 + (v_y + hk_2^{(3)})^2 + (v_z + hk_3^{(3)})^2] / c^2\right)^{1.5} E_x(t + h)$$

$$+\frac{q}{m}\sqrt{1 - [(v_x + hk_1^{(3)})^2 + (v_y + hk_2^{(3)})^2 + (v_z + hk_3^{(3)})^2] / c^2}\left((v_y + hk_2^{(3)})B_z(t + h) - (v_z + hk_3^{(3)})B_y(t + h)\right), \qquad (25)$$

$$k_6^{(4)} = v_z + hk_3^{(3)}. \tag{26}$$

Here, h is the increment of t. The variables at $t + h$ are given as

$$v_x(t+h) = v_x(t) + \frac{1}{6}(k_1^{(1)} + 2k_1^{(2)} + 2k_1^{(3)} + k_1^{(4)}) \tag{27}$$

$$v_y(t+h) = v_y(t) + \frac{1}{6}(k_2^{(1)} + 2k_2^{(2)} + 2k_2^{(3)} + k_2^{(4)}) \tag{28}$$

$$v_z(t+h) = v_z(t) + \frac{1}{6}(k_3^{(1)} + 2k_3^{(2)} + 2k_3^{(3)} + k_3^{(4)}) \tag{29}$$

$$x(t+h) = x(t) + \frac{1}{6}(k_4^{(1)} + 2k_4^{(2)} + 2k_4^{(3)} + k_5^{(4)}) \tag{30}$$

$$y(t+h) = y(t) + \frac{1}{6}(k_5^{(1)} + 2k_5^{(2)} + 2k_5^{(3)} + k_5^{(4)}) \tag{31}$$

$$z(t+h) = z(t) + \frac{1}{6}(k_6^{(1)} + 2k_6^{(2)} + 2k_6^{(3)} + k_6^{(4)}) \tag{32}$$

If the variables at a t are given, then the numerical values at $t + h$ can be obtained from equations (27) – (32), and then the values at $t + 2h$, at $t + 3h$, etc. are obtained by repeating the calculations.

3 Result of the Java Simulation

3.1 Conditions for the Simulation

We consider a simple charge motion injected along the x - direction with the initial velocity $\boldsymbol{v} = (v_0, 0, 0)$ at $\boldsymbol{r} = (0, 0, 0)$ in the alternating electric field, $\boldsymbol{E} = (E_x, 0, 0)$, and the static magnetic field, $\boldsymbol{B} = (0, 0, B_z)$. We use $E_x = E_0\sin(2\pi ft)$, and $B_z = B_0$. Here, E_0 and B_0 are constants, and f is the electric frequency. In this case, the charge moves in the $x - y$ plane and $v^2 = v_x^2 + v_y^2$. If we synchronize the electric field frequency to the frequency f_L of the Larmor motion, $f_L = qB_0/2\pi m^*$, then the charge is continuously accelerated by absorbing energy from the electric field, and its velocity increases with time. The increment functions from equations (11) – (26) for above conditions are given as

$$k_1^{(1)} = \frac{q}{m}\left(1 - (v_x^2 + v_y^2)/c^2\right)^{1.5} E_0 \sin(2\pi ft) + \frac{q}{m}\sqrt{1 - (v_x^2 + v_y^2)/c^2}\, v_y B_0, \tag{33}$$

$$k_2^{(1)} = -\frac{q}{m}\sqrt{1 - (v_x^2 + v_y^2)/c^2}\, v_x B_0, \tag{34}$$

$$k_4^{(1)} = v_x, \tag{35}$$

$$k_5^{(1)} = v_y , \tag{36}$$

$$k_1^{(2)} = \frac{q}{m}\left(1 - \left[(v_x + \frac{hk_1^{(1)}}{2})^2 + (v_y + \frac{hk_2^{(1)}}{2})^2\right] / c^2\right)^{1.5} E_0 \sin[2\pi f(t + \frac{h}{2})]$$

$$+ \frac{q}{m}\sqrt{1 - \left[(v_x + \frac{hk_1^{(1)}}{2})^2 + (v_y + \frac{hk_2^{(1)}}{2})^2\right] / c^2}\left(v_y + \frac{hk_2^{(1)}}{2}\right) B_0 , \tag{37}$$

$$k_2^{(2)} = -\frac{q}{m}\sqrt{1 - [(v_x + \frac{hk_1^{(1)}}{2})^2 + (v_y + \frac{hk_2^{(1)}}{2})^2] / c^2}\left(v_x + \frac{hk_1^{(1)}}{2}\right) B_0 , \tag{38}$$

$$k_4^{(2)} = v_x + \frac{hk_1^{(1)}}{2} , \tag{39}$$

$$k_5^{(2)} = v_y + \frac{hk_2^{(1)}}{2} , \tag{40}$$

$$k_1^{(3)} = \frac{q}{m}\left(1 - \left[(v_x + \frac{hk_1^{(2)}}{2})^2 + (v_y + \frac{hk_2^{(2)}}{2})^2\right] / c^2\right)^{1.5} E_0 \sin[2\pi f(t + \frac{h}{2})]$$

$$+ \frac{q}{m}\sqrt{1 - \left[(v_x + \frac{hk_1^{(2)}}{2})^2 + (v_y + \frac{hk_2^{(2)}}{2})^2\right] / c^2}\left(v_y + \frac{hk_2^{(2)}}{2}\right) B_0 , \tag{41}$$

$$k_2^{(3)} = -\frac{q}{m}\sqrt{1 - \left[(v_x + \frac{hk_1^{(2)}}{2})^2 + (v_y + \frac{hk_2^{(2)}}{2})^2\right] / c^2}\left(v_x + \frac{hk_1^{(2)}}{2}\right) B_0 , \tag{42}$$

$$k_4^{(3)} = v_x + \frac{hk_1^{(2)}}{2} , \tag{43}$$

$$k_5^{(3)} = v_y + \frac{hk_2^{(2)}}{2} , \tag{44}$$

$$k_1^{(4)} = \frac{q}{m}\left(1 - \left[(v_x + hk_1^{(3)})^2 + (v_y + hk_2^{(3)})^2\right] / c^2\right)^{1.5} E_0 \sin[2\pi f(t + h)]$$

$$+ \frac{q}{m}\sqrt{1 - \left[(v_x + hk_1^{(3)})^2 + (v_y + hk_2^{(3)})^2\right] / c^2}\left(v_y + hk_2^{(3)}\right) B_0 , \tag{45}$$

$$k_2^{(4)} = -\frac{q}{m}\sqrt{1-[(v_x+hk_1^{(3)})^2+(v_y+hk_2^{(3)})^2]/c^2}\left(v_x+hk_1^{(3)}\right)B_0, \tag{46}$$

$$k_4^{(4)} = v_x + hk_1^{(3)}, \tag{47}$$

$$k_5^{(4)} = v_y + hk_2^{(3)}. \tag{48}$$

The details of the Java programing for simulating the charge motion using the increment functions are described in Reference [1]. The numerical calculations are performed using the double precision method and using the time increment $h < 0.2m/qB_0$ to obtain an accurate simulation [2].

3.2 Electron Velocity Previously Simulated Using the Invariant Mass

A typical simulation reported previously [2] using the invariant mass for the electron motion with the velocity (v_x: blue line, v_y: red line) accelerated by the synchronized electric field is shown in Figure 1, in which, we use E_0 = 90 V/m, f = 279.92 MHz, and B_0 = 0.01 T, for the electron injected along the x-direction with the initial velocity of 116.8 km/s, consistent with the thermal velocity. In the simulation, the velocity of the electron results in a velocity greater than the velocity of light at the time of 38.5 μs after the injection. In fact, the electron motion near the velocity of light cannot be represented by the classic resonance using the invariant mass, as mentioned in section 2.1. Nevertheless, it is a fact that, if the synchronization is maintained, the electron is accelerated continuously, resulting in a velocity near the velocity of light.

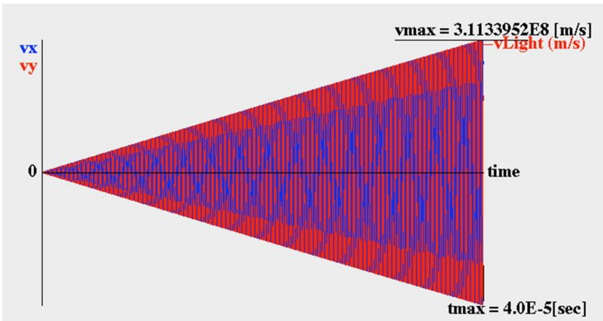

Figure 1: A typical acceleration of the electron by the synchronized electric field to the frequency of the Larmor motion, simulated using the invariant mass. The electron is injected with the initial velocity v_x = 116.8 km/s into the fields at E_0 = 90 V/m, f = 279.92 MHz, and B_0 = 0.01 T. In the simulation, the electron is accelerated up to the velocity of light at t = 38.5 μs after the injection. The velocity of light is shown as vLight in the figure.

3.3 Electron Velocity Simulated Using the Relativistic Mass

In the above simulations, we used the classical model using the invariant mass for the electron motion. As mentioned in section 2.1, a particle moving with a very large velocity behaves effectively as a particle with the relativistic mass. The relativistic mass increases with the increase in the velocity; as a result, the effective Larmor frequency decreases with the increase of the velocity. Therefore, if the value of v/c becomes an effective value to 1 with the increase of the velocity, the applied alternative electric field slips off the synchronization to the frequency of Larmor motion, and the deceleration of the electron becomes superior to the acceleration, resulting in the limitation of the electron velocity. The simulated result using the relativistic mass, that is, using Equations (33) – (48) under the same conditions as those in Figure 1, except for the mass, is shown in Figure 2. The maximum velocity is limited to 1.48 x 10^7 m/sec, that is, the deceleration of the electron becomes dominant at that velocity due to the decrease in the effective Larmor frequency.

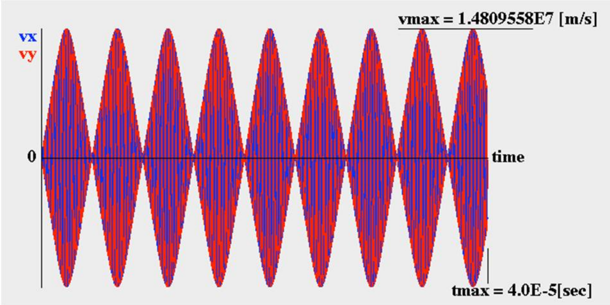

Figure 2: The electron velocity simulated using the relativistic mass under the same conditions as those in Figure 1, except for the mass. The maximum velocity of the electron is limited to 1.48 x 10^7 m/sec.

4 Discussion

The very precise synchronization of the alternative electric field to the frequency of Larmor motion, e.g., six digits of the frequency, is required for the acceleration of the electron near the light velocity, as shown in Figure 1. Therefore, in the use of the relativistic mass, the decrease in the frequency of Larmor motion due to the increase in the velocity is effective at a relatively low velocity, and the electron velocity is limited at the velocity, as shown in Figure 2. In this case, the electron is better accelerated using an initially lower electric frequency than the initially synchronized frequency, taking into consideration of the increase in the relativistic mass, as shown in Figure 3. Even in the case of accounting for the relativistic mass, if the frequency is less than 279.6 MHz, then the alternative electric field slips off the Larmor motion rapidly, and the deceleration becomes immediately dominant, resulting in very little acceleration, as shown in Figure 4. That is, the electron is actually accelerated up to approximately 2.34 x 10^7 m/s at most under these conditions.

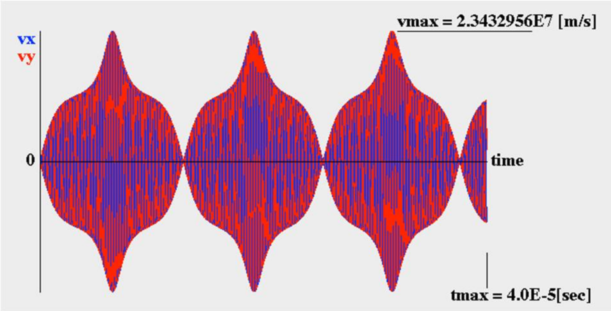

Figure 3: The electron velocity simulated using a slightly lower frequency under the same conditions as those in Figure 2, except the frequency, *f* = 279.6 MHz. The maximum velocity of the electron is limited at 2.34 x 10^7 m/sec, which is 1.6 times larger than the maximum velocity simulated using the initially synchronized frequency, *f* = 279.92 MHz.

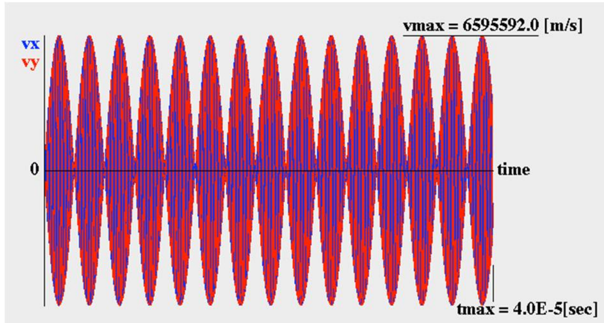

Figure 4: The electron velocity simulated using a slightly lower frequency than 279.6 MHz under the same conditions as those in Figure 3, except the frequency, *f* = 279.5 MHz. The maximum velocity of the electron is limited to a very low velocity, 6.6 x 10^6 m/sec, due the deceleration becoming dominant very rapidly.

5 Conclusion

The numerical simulation of the charge motion near the velocity of light, that is, the charge motion using the relativistic mass by Einstein's special theory of relativity, in electric and magnetic fields was investigated using the fourth-order Runge-Kutta method. The results are summarized as follows:

1. The charge motion can be solved numerically using the incremental functions, Equations (11) – (32).
2. The Larmor motion of the electron in a static magnetic field perpendicularly applied a synchronized electric field was simulated using a Java programing based on the above-described method, resulting in the limitation of the electron velocity at a considerably lower value than the light velocity in contradiction to the previous simulation in which the electron is easily accelerated over the velocity of light due to the use of the invariant mass.

REFERENCES

[1]. Morooka M., Qian S., and Morooka M., *Image Learning of Charge Motion in Electric and Magnetic Fields by Java Programming*, Transactions on Machine Learning and Artificial Intelligence, 2014. 2(2): p. 1-19.

[2]. Morooka M. and Morooka M., *Accuracy of the Java Simulation for the Charge Motion in Electric and magnetic Fields*, Transactions on Machine Learning and Artificial Intelligence, 2015. 3(3): p. 15-23.

[3]. Okun L. B., *The Concept of Mass,* Physics Today, 1989. 42: p. 31-36.